CFD-based analysis of entropy generation in turbulent double diffusive natural convection flow in square cavity

Khaled Said*, *Ahmed* Ouadha, *and Amina* Sabeur.

Laboratoire des Sciences et Ingénierie Maritimes, Faculté de Génie Mécanique, Université des Sciences et de la Technologie Mohamed BOUDIAF d'Oran, Oran El-Mnouar, 31000 Oran, Algérie

Abstract. The present study concerns the problem of natural and double diffusive natural convection inside differentially heated cavity filled with a binary mixture composed of air and carbon dioxide (CO_2). Temperature and CO_2 concentration gradients are imposed on both perpendicular left and right walls. Simulations have been performed using the CFD commercial code *ANSYS* Fluent by solving continuity, momentum, energy and species diffusion equations. Numerical results obtained have been compared to data from the literature for both natural convection thermosolutal cases under laminar and turbulent regimes. For turbulent runs the RNG k-ε model has been selected. A good agreement has been noted between the different types of data for both cases for Rayleigh number ranging between 10^3 and 10^{10} and buoyancy ratio between -5 and +5. Entropy generation rates due to thermal, viscous and diffusive effects have been calculated in post processing for all cases.

1 Introduction

In the last decades great effort has been devoted to the study of natural convection [1-3]. Fluid motion due to pollutant concentration was infrequently taken into account by most of the previous studies. This phenomenon is known as double diffusive convection, also called thermosolutal convection. It has gained researchers interest only in the last few years, due to its importance and utility in multiple fields such as: oceanography, geology, biology, chemical processes, solar engineering equipment's, nuclear reactors, and electronics devices.

Beghein et al. [4] were amongst the earliest researchers who took into account the effect of both thermal and solutal convection inside enclosures. An intensive study was performed in order to determine the influence of a wide range of non-dimensional parameters on double diffusive convection by means of numerical simulation. They concluded that the thermal and solutal *Rayleigh* number beside of *Lewis* number has an observable impact on thermosolutal convection. Koufi et al. [5] carried out CFD numerical simulation in order to investigate laminar double diffusive free convection in square enclosure subjected to uniform temperature and concentration gradients. They found that the thermoslutal flow depends strongly on the buoyancy ratio. Nazari et al. [6] carried out numerical study by means of lattice *Boltzmann* method in order to examine conjugate heat and mass transfer inside cavity occupied with hot square obstacle. The results have demonstrated that the *Nusselt* and *Sherwood* number decrease as the buoyancy ratio rises when N is lower than 1. It was also remarked that they increase as the buoyancy ratio increases in range of $N > 1$. Similar studies have been the subject of several authors [7-8].

Entropy minimization is the main branch in the direction of energy systems designing. It is the most effective way to quantify unavailable energy and work destruction. As a result, an extensive attention was drawn to the topic of entropy generation due to heat and mass transfer. Various studies have been found in the literature dealing with laminar double diffusive convection and entropy generation inside cavities for instance reference [9]. Buoyancy ratio effect on entropy evolution was the subject of multiple authors [10-11]. It was revealed that an increase in buoyancy ratio implies an increase in total entropy generation for thermal dominated flow, while a decrease was observed for solutal dominated flow. In contrast, Oueslati et al. [12] revealed that the total entropy generation decreases as the buoyancy ratio raises regardless the variation of aspect ratio.

Most of the existent studies didn't pay attention to entropy generation under turbulent thermosolutal convection. Even though, Chen and Du [13] as well as Chen et al. [14] explored numerically the entropy generation due to the turbulent thermosolutal free convection. These authors have determined that likewise *Nusselt* and *Sherwood* numbers, the entropy generation was affected by *Rayleigh* number and considerably

* Corresponding author: khalednabil2016@yahoo.com

© The Authors, published by EDP Sciences. This is an open access article distributed under the terms of the Creative Commons Attribution License 4.0 (http://creativecommons.org/licenses/by/4.0/).

improved in turbulent regime and reach its lowest value when $N = 1$.

It is clearly shown from the bibliographic research examined so far, entropy generation on double diffusive natural convection inside square cavity in turbulent regime was handled only by [13] and [14]. Consequently, the present work was conducted aiming mainly to explore entropy generation due to heat and mass transfer inside two dimensional cavity under turbulent flow regime.

2 Mathematical modeling

2.1 Physical problem

The geometric model considered in the present study was the topic of huge interest by numerous authors. It consists of two-dimensional square cavity filled with air or perfect binary gas mixture (air+CO_2). The variation of thermal *Rayleigh* number is defined as function of gravity.

2.2 Governing equations

Continuity, momentum, energy and species diffusion are the equations governing double diffusive natural convection inside enclosures. To simplify the mathematical model, the following approximations are made:

- The fluid is *Newtonian* and incompressible.
- 2D laminar or turbulent flow.
- Absence of radiation.
- The fluid physical properties are constant except density which verifies the *Boussinesq* approximation:

$$\rho(C,T) = \rho_0\left[1 - \beta_T\left(T - T_0\right) - \beta_S\left(C - C_0\right)\right] \quad (1)$$

where thermal and concentration expansion coefficients can be calculated, respectively, as follows:

$$\beta_T = -\frac{1}{\rho_0}\left(\frac{\partial \rho}{\partial T}\right)_{\cdot P,C} \quad (2)$$

$$\beta_S = -\frac{1}{\rho_0}\left(\frac{\partial \rho}{\partial C_0}\right)_{\cdot P,T} \quad (3)$$

2.3 Turbulence modelling

Turbulence occurs in most of engineering applications, thus the choice of turbulence model is the key parameter in order to have accurate results. In the present study the RNG k-ε model was employed to close equations system. This model was highly recommended to handle indoor air flows [15].

2.4 Boundary conditions

The left perpendicular wall of the enclosure is heated (T_H) while the opposite wall is cooled (T_C) with a constant temperature, however the remaining horizontal walls were supposed to be adiabatic with no slip condition imposed. On the other hand, as depicted by Figure 1, the same boundary conditions were set for both, the thermosolutal convection and the natural convection cases. The only exception is that the vertical walls were submitted to contaminant concentration gradients with different locations. The reason behind this is to ensure the variation of the buoyancy forces i.e. aiding or opposing flow.

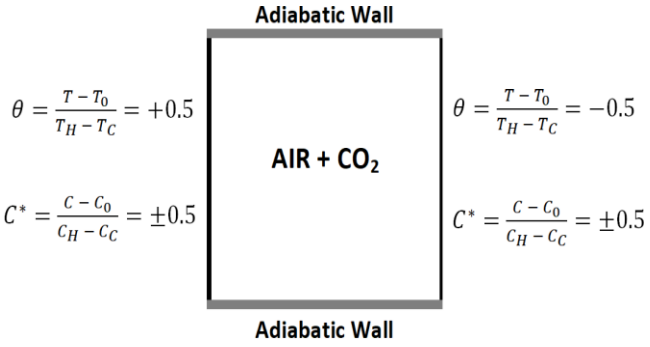

Fig. 1. Geometric model of physical domain with boundary conditions.

2.5 Entropy generation

Entropy generation rate inside two dimensional square cavity filled with *Newtonian* perfect gas mixture with one species diffusion is generated due to friction, heat and diffusion [9]. It can be written as follows:

$$\begin{aligned} S_s = {} & \frac{\mu}{T}\left[2\left(\frac{\partial u}{\partial x}\right)^2 + 2\left(\frac{\partial v}{\partial x}\right)^2 + \left(\frac{\partial u}{\partial y} + \frac{\partial v}{\partial x}\right)^2\right] + \\ & \frac{k}{T^2}\left[\left(\frac{\partial T}{\partial x}\right)^2 + \left(\frac{\partial T}{\partial y}\right)^2\right] + \\ & \frac{R_i D}{C}\left[\left(\frac{\partial C}{\partial x}\right)^2 + \left(\frac{\partial C}{\partial y}\right)^2\right] + \\ & \frac{R_i D}{T}\left[\left(\frac{\partial T}{\partial x}\right)\cdot\left(\frac{\partial C}{\partial x}\right) + \left(\frac{\partial T}{\partial y}\right)\cdot\left(\frac{\partial C}{\partial y}\right)\right] \end{aligned} \quad (4)$$

Bejan number is considered as a good tool in order to determine the dominant between thermal, diffusion, and friction effects on the total entropy. In this case, it is defined as the ratio of entropy due to thermal and diffusive effect over total entropy.

$$Be = \frac{S_{th} + S_{diff}}{S_{th} + S_{fr} + S_{diff}} \quad (5)$$

2.6 Numerical procedure

CFD commercial code *ANSYS* Fluent, based on the finite volume approach, has been used to solve the equations governing the thermosolutal flow inside the cavity (Continuity, momentum, energy and species diffusion equations). For the discretization of the momentum equations, QUICK scheme was employed. However, the discretization of species diffusion, turbulent kinetic energy, and dissipation rate equations terms was ensured by the central upwind second-order scheme. SIMPLEC

was chosen, as the velocity-pressure coupling algorithm while the RNG k-ε turbulence model was selected to handle equations system closure in turbulent regime. The residual error was set to 10^{-7} or less for all cases.

3 Results and discusion

Thermosolutal convection phenomena can be controlled through number of non-dimensionless parameters namely Ra_T, *Le*, *Pr*, and Ra_S or *N*. Each one has a noticeable effect on the flow pattern inside enclosures. The present section deals not only with double diffusive convection, but also with entropy generation due to conjugate heat and mass transfer.

3.1 Mesh study

It should be noted at this level, that a grid independence study is necessary in order to obtain an acceptable CFD numerical solution. For this purpose, various quadratic fine grids were tested to verify the mesh independence towards mean, maximum and minimum *Nusselt* numbers in addition to dimensionless horizontal and vertical velocities components (Nu_{mean}, Nu_{max}, Nu_{min}, U_{max} and W_{max}). Table 1 summarizes the main results:

Table 1. Mesh study for $Ra_T=10^5$.

Mesh	**100 × 100**	**150×150**	**200×200**	**250×250**
Nu_{mean}	4.510	4.518	4.519	4.516
Nu_{max}	7.724	7.720	7.715	7.720
Nu_{min}	0.438	0.633	0.728	0.728
U_{max}	0.130	0.131	0.131	0.131
W_{max}	`0.257	0.257	0.257	0.257

3.2 Validation

The validation of the numerical results is of prime importance for every simulation. For this reason, the verification of our code was built around two different problems reported in the literature. The numerical simulations for the first case consist of two dimensional square enclosure filled with air to handle the issue of free convection in steady laminar and turbulent regime reported by several authors . The second validation correspond to the problem of double diffusive natural convection inside two dimensional square cavity reported by various authors. The computations were verified for different buoyancy ratio in laminar regime.

Table 2 and Table 3 resume simulation results gathered in laminar and turbulent regimes respectively. A wide range of thermal *Rayleigh* number extending from 10^3 to 10^{10} was explored. There is a good match between our results and numerous authors.

Figure 2 illustrate the evolution of local *Nusselt* number alongside the left perpendicular wall versus Beghein et al. [4] numerical results. The outcomes show an excellent agreement.

Table 4 shows the calculated mean *Nusselt* number as function of buoyancy ratio along left vertical wall in laminar regime ($Ra_T=10^7$) .The obtained results agree well enough with various authors and the maximum difference was estimated by only 1% compared to [4].

Table 2. Comparative table of natural laminar convection.

	Present work	**[1]**	**[2]**
Nu_{mean}	1.1176	1.118	1.114
Nu_{max}	1.506	1.505	1.581
Nu_{min}	0.691	0.692	0.670
U_{max}	0.137	0.136	0.153
W_{max}	0.139	0.138	0.155

Table 3. Comparative table of natural turbulent convection.

	Nu_{mean}		
	$Ra_T=10^8$	$Ra_T=10^9$	$Ra_T=10^{10}$
Present work	30.873	59.557	125.880
[2]	32.300	60.100	134.600
[3]	30.506	57.350	103.663

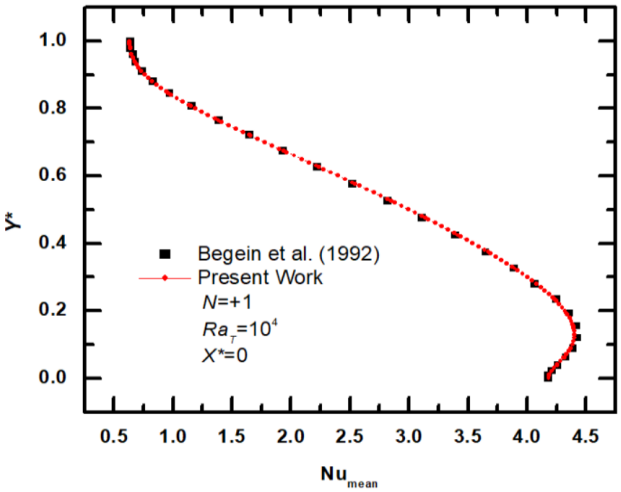

Fig 2. Local *Nusselt* number evolution in laminar regime against Beghein et al. data at $X^*=0$.

Table 4. Mean *Nusselt* number comparison in laminar regime for different buoyancy ratio ($Ra_T=10^7$).

	Nu_{mean}			
N	**Present work**	**[4]**	**[5]**	**[16]**
-0.01	16.47	16.4	13.4	16.3
-0.1	16.06	16.0	16.0	15.9
-0.2	15.56	15.5	15.3	15.4
-0.5	13.72	13.6	13.6	13.5
-0.8	10.69	10.6	10.6	10.5
-0.9	8.82	8.8	8.8	8.6
-1.5	13.72	13.6	13.5	13.5
-5.0	23.80	23.7	23.7	23.6

3.3 Flow characteristics

Figure 3 displays streamlines for high and low thermal *Rayleigh* number. Particular attention was paid to the effect of buoyancy ratio (*N*) in this section. From this figure, it can be seen that the flow is clearly affected with (*N*) variation. Three different flow natures were detected: (a) clockwise motion when thermal buoyancy force is governing, (b) counter-clockwise motion when

the solutal buoyancy force dominates the flow , (c) circular motion at the cavity center when N= -1.

3.4 Heat transfer results

Figure 4 exhibits temperature distribution within square cavity under turbulent and laminar flow regime. It should be pointed out that the same comportment have been found for assisting flow and pure natural convection (N = 0). Right handed flow motion was mentioned. The effect of thermal *Rayleigh* number was significant and the convection was accelerated and amplified in turbulent regime. In contrast, when N=-1, thermal and solutal buoyancy forces are equal but in opposite sign, therefore, they cancelled each other out. This situation leads to convection non-existence and the flow is driven only by diffusion.

3.5 Entropy generation

Figure 5 shows the evolution of total entropy generation as function of buoyancy ratio (N) in laminar and turbulent regime. For turbulent flow, the graphs shows that gradually as the buoyancy ratio increases, the total entropy decreases in range of -5 <N< -1 till reaching its minimum at N= -1 as result of buoyancy force nonexistence. Thus, the obtained results are compatible with reference [11]. The entropy then tends to increase in range of -1 < N < -0.5, to decrease again moderately when -0.5 < N < 0 as consequent of zero diffusive irreversibility. A decrease in total entropy generation was noted as function of buoyancy ratio reduce when N > 0.

Concerning laminar flow (Ra_T =10^3), the outcomes showed that N=0 produces the lowest entropy amongst all cases due to the absence of mass diffusive irreversibility inside the system (almost Zero), and moderate heat irreversibility. When N < 0, the total entropy drop as function buoyancy ratio rises, otherwise it increases. The results also reveal that turbulent regime amplifies the system entropy generation.

Figure 6 depicts a comparison study of *Bejan* number variation in terms of buoyancy forces ratio and *Rayleigh* number in laminar and turbulent regime. The study was conducted in order to highlight the dominance entropy .i.e. Be < 0.5: dominance of fluid friction entropy. Be > 0.5 implies heat and mass transfer entropy dominance.

It is shown that the *Bejan* number remains stable in

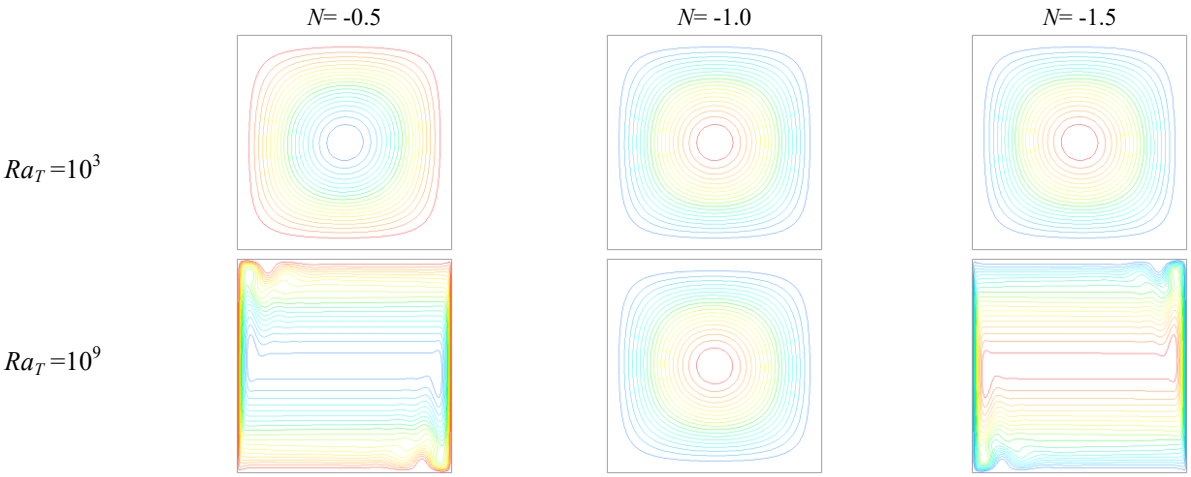

Fig 3. Streamlines for various buoyancy ratio (N) in laminar and turbulent flow.

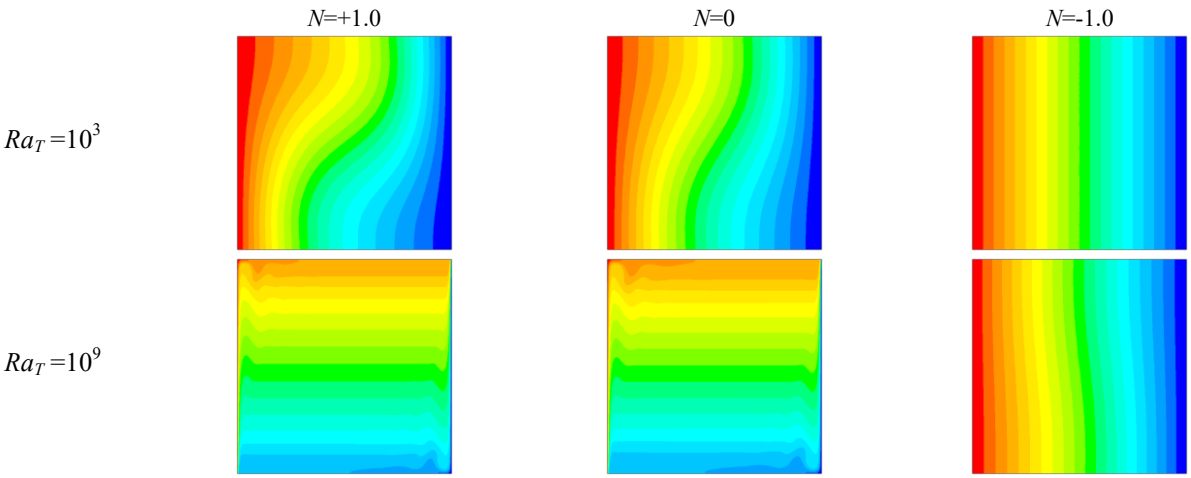

Fig 4. Isotherms (K) for aiding flow (left), pure natural convection (middle), opposing flow (right) under laminar and turbulent flow regime

.

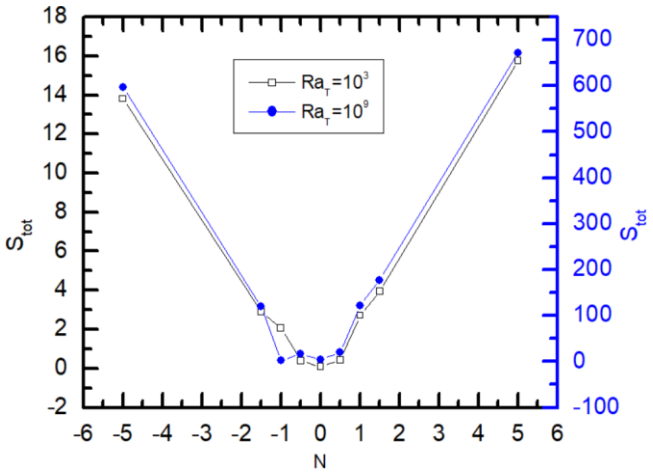

Fig 5. Total entropy variation for different buoyancy ratio (*N*) and thermal *Rayleigh* Number.

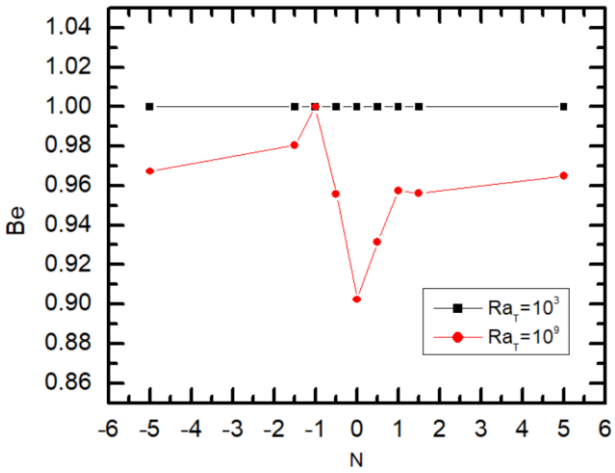

Fig 6. *Bejan* number variation as function of buoyancy ratio (*N*) and thermal *Rayleigh* number.

laminar regime and borders the unity ($Be \simeq 1$) due to the negligibility of friction. *Bejan* number was changed as follow in turbulent regime:

- $-5 < N < -1$: *Bejan* number rise with the increase of buoyancy ratio.
- $-1 < N < 0$: A sudden drop observed as the buoyancy ratio augments.
- $0 < N < +5$: A reduces in *N* decline *Bejan* number.

4 Conclusions

The present paper has proposed numerical solution to the problem of turbulent and laminar double diffusive free convection. Only two articles were found in the literature handled entropy generation in turbulent regime [13-14]. Consequently a numerical investigation was performed pointing mainly to explore entropy generation in turbulent conjugate heat and mass transfer inside square cavity. Various buoyancy ratios were simulated with fixed *Lewis* and *Prandtl* number (*Le*=1 and *Pr* =0.71).

To conclude, the principal findings of this work are listed below:

- CFD codes can be used successfully in order to study natural double diffusive convection.
- Buoyancy forces are cancelled when *N*= -1. As a consequence, the flow is driven only by mass and heat diffusion.
- Entropy generation, *Bejan* and *Nusselt* numbers depend strongly on buoyancy ratio.
- The generation of entropy reaches its lowest point at *N* = -1 and *N*=0 for high *Rayleigh* number and laminar regime, respectively.
- Turbulent flow amplifies entropy generation.

References

1. G. De Vahl Davis, Int. J. Numer. Meth. Fl, **3**, pp. 249-264 (1983)
2. G. Barakos, E. Mitsoulis. D. Assimacopoulos, Int. J. Num. Methods in Fluids, **18**, pp. 695-719 (1994)
3. H.N. Dixit, V. Babu, Int. J. Heat. Mass. Tran, **49**, pp. 727–739 (2006)
4. C. Beghein, F. Haghighat, F. Allard, Int. J. Heat. Mass. Tran, **35**, pp. 833-846 (1992)
5. L. Koufi, L. Cherif, Z. Younsi, H. Naji, Heat Transfer Eng **40,** 15, pp. 1268-1285 (2019)
6. M. Nazari, L. Louhghalam, K. M. Hassan, Chin J. Chem. Eng, **23**, pp. 22-30 (2015)
7. J. Serrano-Arellano, M. Gijón-Rivera, Int. J. Heat. Mass. Tran, **70**, pp. 103-113 (2014)
8. R. Alvarado-Juárez, G. Álvarez, J. Xamán, I. Hernández-López, Desalination, **325**, pp. 84-94 (2013)
9. M. Magherbi, H. Abbassi, N. Hidouri, A. Ben Brahim, Entropy, **8**, pp.1-17 (2006)
10. A. Mchirgui, N. Hidouri, M. Magherbi, Ben Brahim A. Comput Fluids,96, pp.105-115 (2014)
11. Q.Y. Zhu, Y.J. Zhuang, H.Z. Yu, Int. J. Heat. Mass. Tran, **106**, pp.61-82 (2017)
12. F. Oueslati, B. Ben Beya, J Therm Sci Tech-Jpn, **12,** 2 (2017)
13. S. Chen, R. Du, Energy, **36**, 5, pp.1721-1734 (2011)
14. S. Chen, B. Yang, X. Xiao, C. Zheng Int. J. Heat. Mass. Tran, **87**, pp. 447-463 (2015)
15. S. Sadrizadeh, S. Holmberg, AQVEC the 9th International Conference on Indoor Air Quality Ventilation & Energy Conservation In Buildings, Seoul, Republic of Korea, October 23-26 Paper ID: 1018 (2016)
16. J. Xamán, A. Ortiz, G. Álvarez, Y. Chávez, Energy, **36,** 5, pp. 3302-3318 (2011)